AAPS PharmSciTech, Vol. 19, No. 5, July 2018 (© 2018)
DOI: 10.1208/s12249-018-1067-3

Research Article

Preparation and Pharmacokinetics Evaluation of Solid Self-Microemulsifying Drug Delivery System (S-SMEDDS) of Osthole

Chaojie Sun,[1] Yun Gui,[1] Rongfeng Hu,[1,2,5] Jiayi Chen,[3] Bin Wang,[1] Yuxing Guo,[3] Wenjie Lu,[4] Xiangjiang Nie,[1] Qiang Shen,[1] Song Gao,[1] and Wenyou Fang[1]

Received 17 January 2018; accepted 2 May 2018; published online 29 May 2018

Abstract. The study was performed aiming to enhance the solubility and oral bioavailability of poorly water-soluble drug osthole by formulating solid self-microemulsifying drug delivery system (S-SMEDDS) *via* spherical crystallization technique. Firstly, the liquid self-microemulsifying drug delivery system (L-SMEDDS) of osthole was formulated with castor oil, Cremophor RH40, and 1,2-propylene glycol after screening various lipids and emulsifiers. The type and amount of polymeric materials, good solvents, bridging agents, and poor solvents in S-SMEDDS formulations were further determined by single-factor study. The optimal formulation contained 1:2 of ethyl cellulose (EC) and Eudragit S100, which served as matrix forming and enteric coating polymers respectively. Anhydrous ethanol and dichloromethane with a ratio of 5:3 are required to perform as good solvent and bridging agent, respectively, with the addition of 0.08% SDS aqueous solution as poor solvent. The optimized osthole S-SMEDDS had a high yield (83.91 ± 3.31%) and encapsulation efficiency (78.39 ± 2.25%). Secondly, osthole L-SMEDDS was solidified to osthole S-SMEDDS with no significant changes in terms of morphology, particle size, and zeta potential. *In vitro* release study demonstrated a sustained release of the drug from osthole S-SMEDDS. Moreover, *in vivo* pharmacokinetic study showed that the T_{max} and mean residence time ($MRT_{(0\text{-}t)}$) of osthole were significantly prolonged and further confirmed that osthole S-SMEDDS exhibited sustained release effect in rabbits. Comparing with osthole aqueous suspension and L-SMEDDS, osthole S-SMEDDS increased bioavailability by 205 and 152%, respectively. The results suggested that S-SMEDDS was an effective oral solid dosage form, which can improve the solubility and oral bioavailability of poorly water-soluble drug osthole.

KEY WORDS: osthole; self-microemulsion; spherical crystallization technique; bioavailability.

INTRODUCTION

Osthole, a natural coumarin compound, is an extract from the fruits of *Cnidium monnieri* (L.) Cusson. In recent years, there has been a growing interest in osthole because of the impacts it has on the cardiovascular system (1), central nervous system (2), immune system (3), tumor (4), osteoporosis (5,6), and other aspects (7). However, its poor water solubility (~ 0.63 mg/L), pH sensitivity (8), and poor oral absorption (9–12) significantly prevent osthole from achieving useful clinical applications. Therefore, it is of great importance to develop an appropriate dosage form for osthole.

To date, a number of pharmaceutical methods (13–22), which are especially liquid self-microemulsifying drug delivery system (L-SMEDDS), have been developed as viable drug delivery approaches to address the abovementioned problems.

L-SMEDDS promotes drug absorption through intestinal lymph, avoiding the first pass effect of drugs. Moreover, drug delivered by L-SMEDDS can spontaneously form microemulsion with droplet size of dozens of nanometers in the gastrointestinal tract after oral administration (23–26) and hence improve the absorption and bioavailability of poorly water-soluble drugs (27). Despite the above advantages, L-

Chaojie Sun and Yun Gui contributed equally to this work.

[1] Key Laboratory of Xin'an Medicine, Ministry of Education, Anhui Province, Key Laboratory of R&D of Chinese Medicine, Anhui University of Traditional Chinese Medicine, Hefei, 230038, Anhui, People's Republic of China.
[2] Anhui "115" Xin'an Medicine Research & Development Innovation Team, Hefei, 230038, Anhui, People's Republic of China.
[3] Department of Pharmaceutical Sciences, College of pharmacy and Health Sciences, St. John's University, Jamaica, New York 11439, USA.
[4] School of Pharmacy, China Pharmaceutical University, Nanjing, 210009, Jiangsu, People's Republic of China.
[5] To whom correspondence should be addressed. (e–mail: rongfenghu2003@hotmail.com)

SMEDDS also has some major drawbacks such as long-term stability issue, storage and transportation inconvenience, and irreversible drug precipitation.

To overcome these problems, liquid formulations can be transformed to solid dosage forms by suitable methods. A variety of curing solidification methods have been explored, extrusion roll method (28), spray drying method (29,30), solid carrier adsorption method (31), and so on (32). Nevertheless, these curing methods require harsh preparation conditions. For example, extrusion roll method and spray drying method involve high temperature which may be infeasible for heat-sensitive drugs. Also, high temperature influences the drug loadings due to the decrease of the volatile surfactant in L-SMEDDS. On the other hand, solid carrier adsorption requires a large amount of adsorbent, which may lead to high viscosity and low drug loading capacity. Thus, a more efficient method for curing L-SMEDDS is urgently demanded.

As a part of our long-term interest in solving the oral bioavailability of poorly soluble drug (27,33,34), we solidified the L-SMEDDS into solid self-microemulsifying drug delivery system (S-SMEDDS) by applying spherical crystallization technique, which was a one-step solidification method that was executed in the liquid phase. Spherical crystallization may occur *via* two mechanisms: spherical agglomeration (SA) and emulsion solvent diffusion (ESD). And the agglomeration process principally requires a three-solvent system, *i.e.*, a liquid bridge agent, a good solvent, and a poor solvent. In this study, the agglomeration process could be carried out using the emulsion-solvent-diffusion method. When the good solvent solution of the drug was poured into the poor solvent under agitation, due to the strong interaction between the drug and the good solvent, the drug solution formed quasi-emulsion droplets and dispersed in the poor solvent. By the diffusion of the good solvent in the poor solvent, crystallization occurred in the droplets. The liquid bridging agent agglomerated the precipitated crystals (35–38). In particular, this solidification method features simple operation, high drug encapsulation efficiency, low cost, and elimination of high temperature (39,40).

In this study, we developed the osthole S-SMEDDS from osthole L-SMEDDS by applying spherical crystallization technique. The micromeritic properties, particle size, and morphology were assessed to optimize the formulation and processing parameters. The *in vitro* release and stability studies were also conducted. In addition, the pharmacokinetics parameters including oral bioavailability of osthole S-SMEDDS were determined in comparison with the drug suspension and the L-SMEDDS.

MATERIALS AND METHODS

Materials

Osthole (98.5%) was purchased from Yuanye Biological Technology Co., Ltd. (Shanghai, China). Cremophor RH40 was obtained from Haian Petrochemical Plant (Jiangsu, China). Castor oil was purchased from Damao Chemical Reagent Factory (Tianjin, China). Solutol HS15 was purchased from Fenglijingqiu Trading Co., Ltd. (Beijing, China). Tween80 was obtained from Guangfu Fine Chemical Research Institute (Tianjin, China). 1,2-Propylene glycol was purchased from Suyi Chemical Reagent Co., Ltd. (Shanghai, China). Eudragit S100 was kindly provided by Evonik Company (Essen, Germany). Hydroxypropyl methylcellulose phthalate HP55 (HPMCP-HP55) was gifted from Shin-Etsu Chemical Co., Ltd. (Tokyo, Japan). Cellulose acetate (CA) and ethyl cellulose (EC) were supplied by Sinopharm Chemical Reagent Co., Ltd. (Shanghai, China). Micro silica was gifted from Sunhere Pharmaceutical Excipients Co., Ltd. (Anhui, China). Sodium dodecyl sulfate (SDS) was bought from Sinopharm Chemical Reagent Co., Ltd. (Shanghai, China). All other reagents were of analytical grade, and deionized double-distilled water was used throughout the study.

Solubility Studies

To select a suitable oil and emulsifier for L-SMEDDS, the solubility of osthole in various oils and surfactants was measured. Briefly, an excessive amount of osthole was added to the oils (ethyl oleate, soybean oil, castor oil) and emulsifiers (RH40, HS15, Tween80), respectively. The mixture was stirred overnight and centrifuged at 3000*g* for 10 min. From each sample, 100-μL supernatant was collected and diluted with acetonitrile to 100 mL. The solution was filtered through a 0.45-μm membrane filter. The drug concentration in the solution was analyzed by an HPLC method on an Agilent 1260 HPLC system (Agilent, USA). Forty microliters of sample was injected for each analysis by HPLC method on an Agilent 1260 (Agilent, USA) HPLC system. The solubility studies were carried out in triplicate.

Preparation of Osthole L-SMEDDS

The osthole L-SMEDDS containing castor oil, Cremophor RH40, and 1,2-propylene glycol has been developed. Osthole (50 mg) was dissolved completely in preheated 54.1% Cremophor RH40 at 37°C by ultrasonic method, and 10.5% castor oil and 32.4% 1,2-propylene glycol were then added. The prepared osthole L-SMEDDS was diluted with pH 6.8 PBS to form microemulsion. Droplet size and zeta potential of the microemulsion were measured by a Malvern Nano ZS90 particle size analyzer (Malvern, UK).

Influence of pH, Dilution Times, and Rotation Rate on L-SMEDDS Emulsification Time

pH of Media

One milliliter of osthole L-SMEDDS was diluted to 50 mL by double-distilled water, 0.9% sodium chloride solution, hydrochloric acid (0.1 M), and pH 6.8 phosphate-buffered saline (PBS), respectively. The mixture was stirred at 200 rpm. The end of emulsification was determined by visual observation and the time was recorded.

Dilution Times

One milliliter of osthole L-SMEDDS was diluted with pH 6.8 PBS to 10, 25, 50, 100, and 150 times, respectively. The

mixture was stirred at 150 rpm. Time for emulsification was recorded when the mixture became clear and transparent.

Stirring Speed

One milliliter of osthole L-SMEDDS was added into 50 mL of pH 6.8 PBS. The mixture was stirred at 50, 100, 150, and 200 rpm, respectively. The time required for the complete emulsification was determined in the same manner as above.

Preparation and Evaluation of Osthole S-SMEDDS

Four polymers, including Eudragit S100, EC, CA, and HPMCP-HP55, were selected. Good solvents in this experiment were ethanol, methanol, acetonitrile, tetrahydrofuran, acetone, and acetic acid while dichloromethane, ethyl acetate, petroleum ether, *n*-butanol, ether, and *n*-hexane were evaluated as bridging agents. A certain amount of various polymers was dissolved in various combinations of good solvents and bridging agents. The selected osthole L-SMEDDS and the polymer solution were then quickly added into the poor solvent, respectively. The mixture was stirred until complete separation of the microspheres (osthole S-SMEDDS). Osthole S-SMEDDS was then collected and filtered through a sieve (80 meshes). The product was air-dried to a constant weight over several days before weighing. The dried products were stored in a vacuum dryer at room temperature before further use.

Spherical Formation and Yield

The osthole S-SMEDDS prepared *via* the spherical crystallization technique was evaluated by optical observation in an N-108M optical microscope (Ningbo, China) to determine whether microspheres formed after drying. Yield was calculated according to the following formula:

$$\text{Yield}(\%) = M_1 \div M_0 \times 100\%$$

where M_1 represents the weight of the microspheres after drying and M_0 represents the total weight of the osthole L-SMEDDS and the macromolecule polymeric materials.

Carr's Index

Carr's index (CI) is normally used to reflect the compressibility of the powder. The compressibility index and flowability of the crystal have a close relevancy (41,42). The bulk and tapped densities of the osthole S-SMEDDS were measured. The CI was computed by the following equation:

$$\text{CI} = (1-\rho_0/\rho_f) \times 100\%$$

where ρ_o and ρ_f are tapped density and bulk density, respectively.

Angle of Repose

The angle of repose was measured by the funnel method (43). Briefly, a certain amount of S-SMEDDS particles was flowed out uniformly from the funnel at a certain oscillation frequency until the formed microsphere cone reached the highest height. The angle between the cone and plane is the angle of repose. The height of the cone (h) and the radius of the basal plane (r) were measured, and the angle of repose (α) was determined by the following equation:

$$\alpha = \tan^{-1}(\text{h/r.})$$

Optimization of Formulation and Processing Parameters

The formulation and processing parameters of osthole S-SMEDDS were optimized by a single-factor test. The single factors tested were as follows: type of polymer material, type of good solvents and bridging agents, type of poor solvents, and stirring speed, temperature, and time.

Determination of Encapsulation Efficiency

An appropriate amount of the osthole S-SMEDDS was washed with distilled water and sieved (80 meshes) to remove the unencapsulated drug. And then, the microspheres were dissolved completely in ethanol by ultrasound. The solution was filtered and the total amount of encapsulated drug in the microspheres was determined by HPLC. Drug encapsulation efficiency (EE) was calculated as follows:

$$\text{EE}(\%) = W_t/W_d \times 100\%$$

where W_t is the encapsulated amount and W_d is the total amount of osthole added in the S-SMEDDS.

Morphological Analysis

Transmission electron microscopy (TEM) was conducted by the negative staining method to evaluate the L-SMEDDS and S-SMEDDS of osthole. The L-SMEDDS and S-SMEDDS of osthole were diluted 50-fold with pH 6.8 PBS to form the microemulsion before the TEM study. And then, a drop of microemulsion was applied on a carbon-coated copper grid (200–300 meshes) and stained with 1% phosphotungstic acid (PTA). After drying, the morphology of the osthole L-SMEDDS and S-SMEDDS was visualized using TEM (Hitachi H-7650, Japan) at 5000–50,000 magnification with an accelerating voltage of 80 kV. Scanning electron microscopy (SEM) was also utilized to evaluate the osthole S-SMEDDS.

***In Vitro* Release**

In most cases, the *in vitro* release tests of oral preparations are carried out in media simulating the gastrointestinal fluids. Due to the instability of osthole in the acidic

environment, the enteric preparations were prepared and their release tests were performed with accordance to the basket method described in the 15th edition of the Chinese Pharmacopoeia. The release media were 0.1 M hydrochloric acid for the first 2 h and pH 6.8 PBS for the rest of the study. Both the media contained 40% ethanol to facilitate the release of the drug. During the experiment, the temperature and the stirring speed were kept at 37 ± 0.5°C and 100 rpm, respectively. An appropriate amount of the osthole S-SMEDDS was placed in a dialysis bag (cut off MW 8000–14,000, VISKASE® Companies Inc., USA) which was submerged in 900 mL of the release media. Five milliliters of sample was withdrawn at 0.17, 0.25, 0.33, 0.5, 1, 1.5, 2, 3, 4, 5, 6, 8, 10, and 12 h. The media was replenished with the equivalent volume of fresh isothermal hydrochloric acid or PBS, respectively, after each sampling. The samples were then filtered through a 0.45-μm membrane filter before analyzed by HPLC. The percentage cumulative release at time t was calculated as follows:

$$\text{Cumulative release percentage} = \left(C_t \times V_0 + \sum_{n=1}^{t=1} C_n \times V\right)/M_0 \times 100\%$$

where C_t is the concentration at time t, V_0 and V are the total volume of release medium and sample volume, respectively, and M_0 is the total amount of the drug in the microspheres.

Preliminary Stability Study

Osthole has a lactone structure which is subject to slow esterification in acidic aqueous condition. Thus, the stability study was conducted to evaluate the decomposition of osthole and its leakage from the S-SMEDSS. Briefly, the osthole S-SMEDDS was tested under stressed temperatures (4 and 60°C), high relative humidity (92.5% RH), and strong light exposure (4500 lx). Moreover, 6-month storage under accelerated conditions (40°C, 75% RH) was also conducted. The stability of the S-SMEDDS was determined by the indicators including droplet size of the microemulsion formed by the diluted osthole S-SMEDDS, morphological appearance, and encapsulation efficiency of osthole S-SMEDDS.

In Vivo Pharmacokinetics Study

Male New Zealand rabbits (2.5 ± 0.2 kg) were purchased from the Laboratory Animal Center of Anhui Medical University (Hefei, China). The animal experiments were approved and supervised by the Animal Experimental Ethical Committee of Anhui Medical University (Hefei, China). These rabbits were fed with standard diet and had free access to distilled water. They were fasted overnight prior to the experimental and were randomly divided into three groups (three animals per group). A single dose (50 mg/kg) of osthole aqueous suspension, or osthole L-SMEDDS and osthole S-SMEDDS was administrated orally to each animal of different groups (L-SMEDDS and S-SMEDDS were mixed homogeneously with 10 mL distilled water before dosing). Blood samples (0.5 mL each) were collected through the peripheral ear vein into heparinized tubes at 0.25, 0.5, 1, 2, 3, 4, 5, 6, 8, 12, and 24 h after dosing. Then, the blood samples were centrifuged at 3000*g* for 10 min. The supernatant plasma was stored at − 20°C for further analysis.

To analyze the drug concentration in the plasma samples, 200 μL of each of the samples was placed in a centrifugal tube and 100 μL acetonitrile was added into it. After being vortexed for 2 min and centrifuged at 5000*g* for 15 min, 40 μL of the supernatant was analyzed by HPLC on an Agilent 1260 HPLC system (Agilent, USA) with a XB-C_{18} column (4.6 × 250 mm, 5 μm) at 25°C. The mobile phase was composed of acetonitrile and water (60:40, *v*/*v*). The eluent was monitored at 322 nm with a flow rate of 1.0 mL/min.

Statistical Analysis

The DAS 2.0 pharmacokinetics software was used to calculate the pharmacokinetic parameters. All data in this study were expressed as mean ± standard deviation. The acquired data were analyzed by one-way analysis of variance (ANOVA).

RESULTS AND DISCUSSIONS

Solubility Studies

Various oils and surfactants were screened for their solubilizing capacity for osthole. Among the ingredients tested (Fig. 1), osthole showed higher solubility in castor oil (19.88 ± 1.17 mg/mL) than in soybean oil (15.32 ± 2.98 mg/mL) or ethyl oleate (14.60 ± 1.02 mg/mL). The drug solubility in selected emulsifiers followed the order of Cremophor RH40 (25.15 ± 1.37 mg/mL), Tween 80 (22.15 ± 1.58 mg/mL), and Solutol HS15 (19.12 ± 1.11 mg/mL), from highest to lowest. The solubility of osthole in castor oil was statistically different with the solubility of osthole in soybean oil or ethyl oleate ($p < 0.05$). The solubility of osthole in Cremophor RH40 was statistically different with Tween 80 ($p < 0.05$) and Solutol HS15 ($p < 0.01$). Co-emulsifiers were also studied (results not shown), and 1,2-propylene glycol (57.96 ±

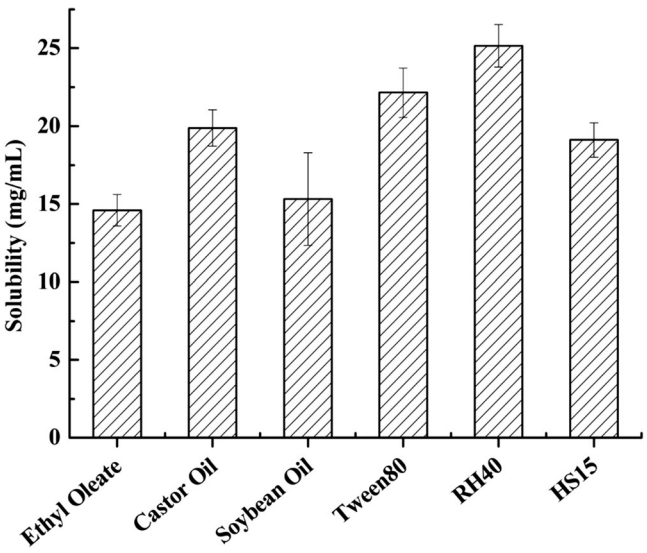

Fig. 1. Solubility of osthole in various vehicles (mean ± SD, $n = 3$)

1.70 mg/mL) was selected due to its high solubilizing capacity for osthole without impacting the emulsification process.

Preparation and Evaluation of Osthole L-SMEDDS

Droplet Size and Zeta Potential of Osthole L-SMEDDS

The microemulsion by the diluted osthole L-SMEDDS was clear and transparent with slightly blue opalescent under light. No turbidity or phase separation was observed during the storage at room temperature. The average droplet size and the zeta potential were 22.76 nm and −2.77 mV, respectively (Fig. 2).

Influence of pH, Dilution Time, and Stirring Rate on Osthole L-SMEDDS Emulsification Time

It was demonstrated that the tested media had no influence on the emulsification rate of the L-SMEDDS. However, the self-emulsifying time was shorted and the greater the stirring rate, the shorter the self-emulsifying time. Besides, there had no impact of dilution on droplet size if the dilution time reached 50 or above. When the dilution time was insufficient, the L-SMEDDS could not fully self-emulsify, resulting in aggregation. On the other hand, when the dilution time was overly large, the zeta potential of the microemulsion by the osthole L-SMEDDS would go infinitely close to zero. The results suggest that the osthole L-SNEDDS was stable in the dilution range of 10–150 times.

Preparation and Evaluation of Osthole S-SMEDDS

Screening of Polymeric Materials. The polymeric materials play an important role in the formation of microspheres and drug release. Taking the pH sensitivity of osthole in gastric juice into account, application of enteric coating played a key role in solving the problem (44–47). In the current study, four polymers, including Eudragit S100, EC, CA, and HPMCP-HP55, were evaluated based on sphere formation and product yield. The results show that CA could not help to form microspheres. These microspheres formed by HPMCP-HP55 had rough surfaces and various sizes. EC and Eudragit S100 produced microspheres with high yield (87.5 and 77.2%, respectively). Therefore, EC was selected to be combined with Eudragit S100, which served as the enteric coating material. Further study revealed that with the increase in the ratio of EC: Eudragit S100, the surface of the microspheres became rougher, and the drug release was faster possibly due to the more porous shell. Contrarily, the yield of microspheres was lower with the increase in proportion of Eudragit S100. Considering the balance between the yield and release profile, the optimal ratio of EC, Eudragit S100 was found to be 1:2.

Selecting of Good Solvents and Bridging Agents. Whether the good solvents and the bridging agents are miscible with each other and able to dissolve the polymer directly affects the formation of S-SMEDDS. Pre-experimental results in our lab suggest that the combination of ethanol and *n*-butanol could not dissolve the polymer. Methanol and petroleum ether were not miscible, neither were the combination of acetonitrile, petroleum ether, nor *n*-hexane. The results are summarized in Table I. The combination using ethanol and dichloromethane, acetonitrile and dichloromethane, and tetrahydrofuran and petroleum ether resulted in high yield, *i.e.*, 85.2, 83.4, and 82.5%, respectively. However, the shells of the microspheres prepared by acetonitrile and methylene chloride, or tetrahydrofuran and petroleum ether as respective good solvents and bridging agents had too many pore. Therefore, the optimized system utilized anhydrous ethanol and dichloromethane. It was also found that a 5:3 ratio of ethanol *versus* dichloromethane resulted in the maximum yield (Table II).

Influence of Poor Solvents. The poor solvents were critical in the formation of spheres (48,49). It was found that liquid paraffin and 0.08% sodium dodecyl sulfate (SDS) aqueous solution could turn the polymer into a solid ball in the prior experiment without having significant impacts on yield, Carr's index, and angle of repose. In consideration of the cost, 0.08% SDS aqueous solution was finally selected as the poor solvent. It was demonstrated that the volume of 0.08% SDS aqueous solution had profound effect on forming microspheres. When the volume of 0.08% SDS aqueous solution used is too small or too large, the polymer cannot be incorporated into the microspheres. The reason may be that

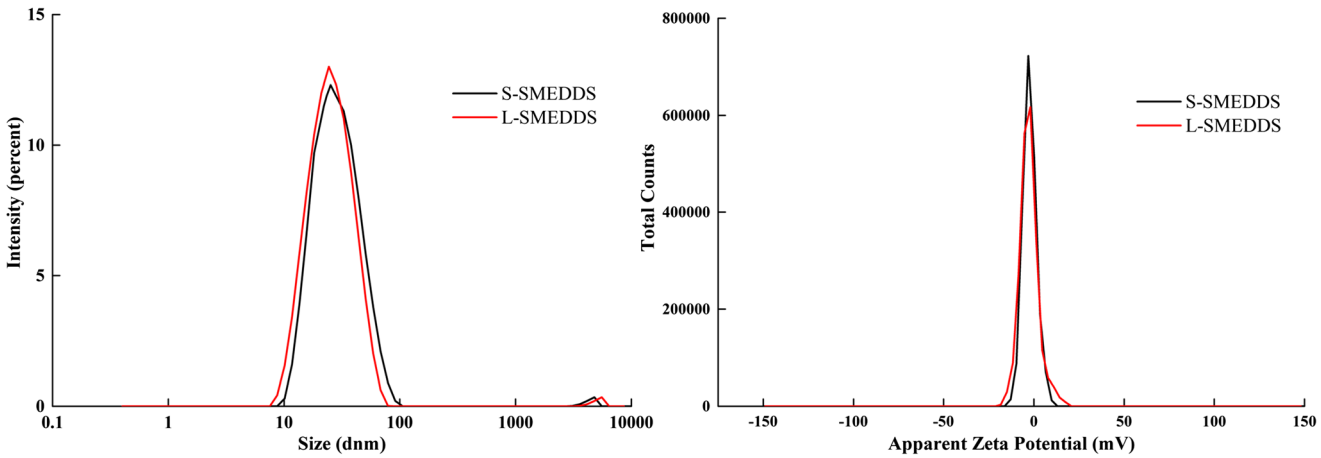

Fig. 2. Particle size and zeta potential of osthole L-SMEDDS and osthole S-SMEDDS

Table I. Effects of Types of Good Solvents and Bridging Agents on the Microspheres (Mean ± SD, $n = 3$)

Good solvents	Bridging agents	Angle of repose (°)	Carr's index (%)	Yield (%)
Methanol	Dichloromethane	26.3 ± 1.2	18.3 ± 0.6	78.4 ± 2.1
Ethanol	Dichloromethane	24.3 ± 1.1	18.2 ± 1.5	85.2 ± 1.4
Acetonitrile	Dichloromethane	31.5 ± 0.6	19.4 ± 0.8	83.4 ± 1.8
	Ethyl acetate	25.8 ± 0.5	20.3 ± 1.1	69.6 ± 1.2
Tetrahydrofuran	Dichloromethane	24.2 ± 0.7	17.3 ± 0.5	70.5 ± 3.4
	Ethyl acetate	23.8 ± 1.7	19.6 ± 1.4	70.6 ± 2.5
	Petroleum ether	21.6 ± 0.9	21.6 ± 1.0	82.3 ± 3.9
	n-butanol	19.3 ± 0.5	23.4 ± 2.2	76.4 ± 1.7
Acetone	Dichloromethane	24.7 ± 1.0	21.2 ± 1.4	63.5 ± 0.9
	Ethyl acetate	19.2 ± 0.3	16.6 ± 0.8	67.7 ± 3.5
Acetic acid	Dichloromethane	25.3 ± 2.1	17.3 ± 1.0	55.4 ± 2.3

when the volume used was too small, the organic solvent would spread so slowly that emulsion droplets aggregated and were too big to be a microsphere, and when the volume was too large, the organic solvent spread too fast to make the polymer form valid emulsion droplets. From the yield and other evaluation indicators, the volume of 0.08% SDS aqueous solution was 120 mL.

In summary, the optimized formulation was composed of EC and Eudragit S100 (1:2). Anhydrous ethanol and dichloromethane (5:3) were used as the good solvent and bridging agent, respectively. One hundred twenty milliliters of 0.08% SDS solution served as the poor solvent. The preparation condition was set up as 400-rpm stirring for 35 min at 25°C. The osthole S-SMEDDS prepared according to the optimized formulation and preparation parameters had a yield of 83.91 ± 3.31% and encapsulation efficiency of 78.39 ± 2.25% with good reproducibility.

Particle Size and Zeta Potential

The results showed that the mean particle size and zeta potential of the microemulsion released from the osthole S-SMEDDS were 23.35 nm and − 1.80 mV, respectively (Fig. 2). This was consistent with the data acquired from the osthole L-SMEDDS where the particle size was 22.76 nm, and the zeta potential was − 2.77 mV, indicating that the osthole L-SMEDDS had not been destroyed during the curing process.

Morphological Analysis

Morphological characterization of the osthole L-SMEDDS and S-SMEDDS is shown in Fig. 3. The TEM pictures reveal that the osthole L-SMEDDS (Fig. 3a) and osthole S-SMEDDS (Fig. 3b) were similar in appearance and size. The results further indicate that the curing process by spherical crystallization technique had no significant impact on the droplet size. The SEM picture (Fig. 3c) shows the osthole S-SMEDDS displaying spherical shape with a relatively smooth surface and uniform size at different magnifications.

In Vitro Release

As it is shown in Fig. 4, the osthole S-SMEDDS released about 15% of the drug in the first 2 h and a complete release was achieved in 8 h. The release profile indicates a sustained release effect. When fitted to various models including first-order, Higuchi, and zero-order kinetics, the release profile fitted the first-order best (Table III). The release curves of the L-SMEDDS and S-SMEDDS in acidic pH were compared (Fig. 5). There was 95% drug release from osthole L-SMEDDS within 2 h while only about 15% release from the S-SMEDDS. It may be due to that the L-SMEDDS can quickly enter into the simulated gastric juice and form nanosize emulsion droplets (16). However, osthole S-SMEDDS was firstly dissolved into osthole L-SMEDDS, and then the existence of the enteric polymer also prevented the release of osthole in simulated gastric juice (50). In this

Table II. Effects of Amount of Good Solvents and Bridging Agents on the Microspheres (Mean ± SD, $n = 3$)

Ethanol:dichloromethane	Morphological appearance	Angle of repose (°)	Carr's index (%)	Yield (%)
2:6	0	N/A	N/A	N/A
3:5	0	N/A	N/A	N/A
4:4	1	19.2 ± 1.5	23.5 ± 0.7	47.8 ± 2.1
4:3	1	22.4 ± 1.1	21.6 ± 2.4	56.8 ± 3.5
5:3	1	26.7 ± 0.9	20.1 ± 1.6	81.2 ± 2.5
6:2	0	N/A	N/A	N/A
5:1	0	N/A	N/A	N/A

"1" means the particle was spherical shape, and "0" means the particle was not spherical shape. "N/A" represents not applicable

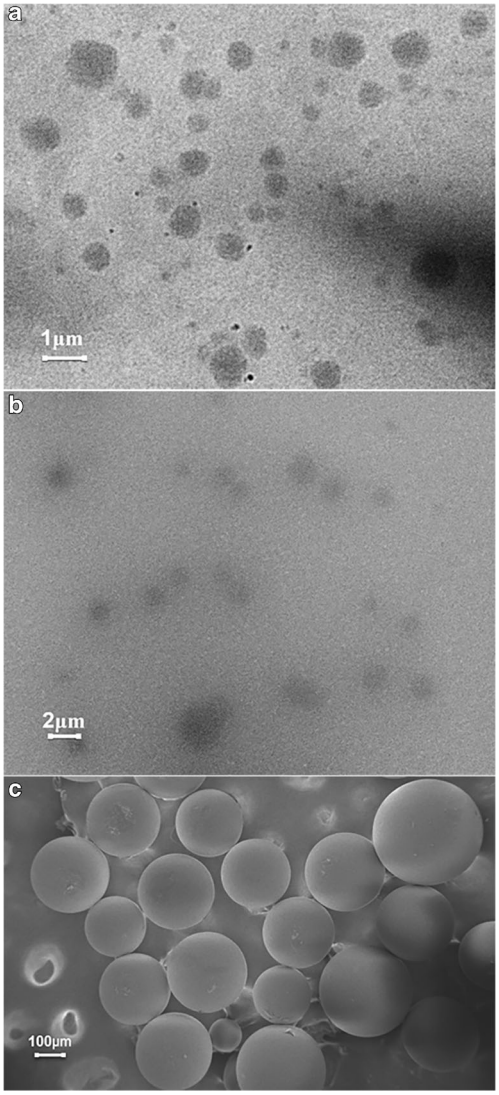

Fig. 3. TEM of osthole L-SMEDDS (**a**) and osthole S-SMEDDS (**b**), SEM of osthole S-SMEDDS (**c**)

Table III. Model Fitting for *In Vitro* Release Profile of Osthole S-SMEDDS

Model	Fitted equation	*R*
Zero-order model	$Q = 15.889t - 7.8517$	0.9741
First-order model	$Q = -0.5727t_{1/2} + 1.209$	0.9908
Higuchi model	$In(1 - Q) = 0.2404t + 0.0846$	0.9885

case, due to the pH sensibility of osthole, osthole S-SMEDDS had a better *in vitro* release than osthole L-SMEDDS.

Preliminary Stability Study

Slight oil leakage and reduced entrapment efficiency were observed at high temperature (60°C), high relative humidity (92.5%), and strong light exposure (4500 lx). The accelerated test showed that after 3 months, the particle size and the entrapment efficiency were 25.94 ± 0.27 nm and 45.12% ± 0.45%, respectively. There was no obvious change with the appearance in 3 months under accelerated conditions (40°C, 75% RH). It indicated that osthole S-SMEDDS was uniform and stable. And for the last 3 months, the microspheres gradually gathered into cluster; particle size and entrapment efficiency could not be measured easily. These results show that the osthole S-SMEDDS was sensitive to temperature and moisture. When stored at low temperature (4°C) for 10 days, the osthole S-SMEDDS showed no change in size or encapsulation efficiency. These results suggest that the preparation should be stored sealed at low temperature and protected from light.

In Vivo Pharmacokinetics Study

Pharmacokinetic studies were carried out in rabbits (28,51), the mean plasma concentration *vs.* time profiles are illustrated in Fig. 6, and the pharmacokinetics parameters are presented in Table IV. A significant increase in $AUC_{(0\text{-}t)}$ could be found when S-SMEDDS was compared with either suspension (2.05 times increase) or L-SMEDDS (1.52 times

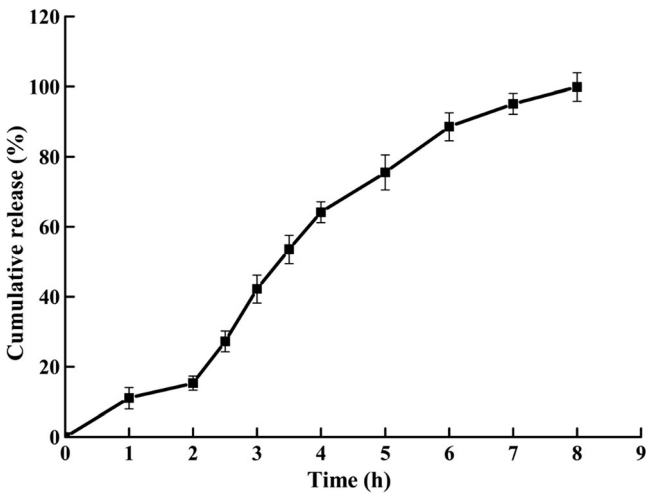

Fig. 4. Cumulative percentage release of osthole S-SMEDDS (mean ± SD, $n = 6$)

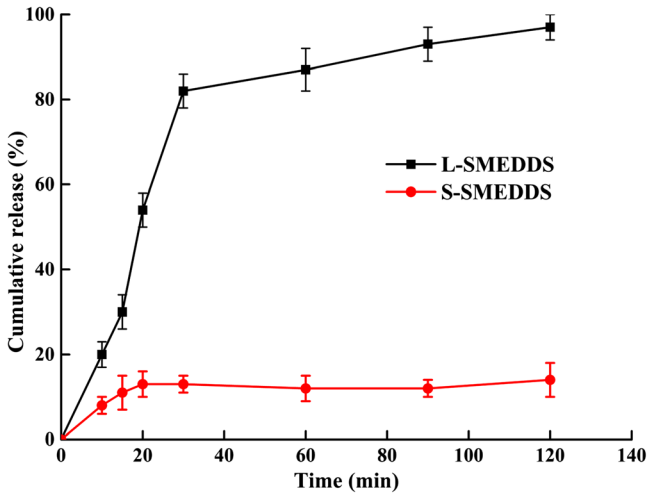

Fig. 5. Release of osthole L-SMEDDS and S-SMEDDS in 0.1 M hydrochloric acid (mean ± SD, $n = 6$)

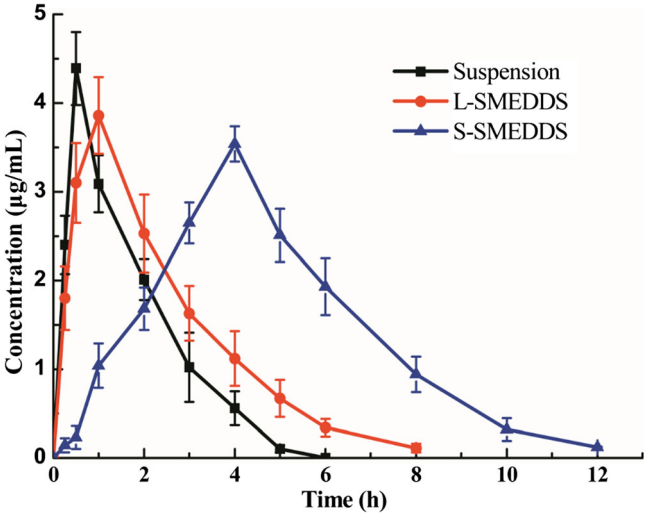

Fig. 6. Concentration-time curve of osthole S-SMEDDS, osthole L-SMEDDS, and osthole aqueous suspension in rabbits after a single oral dosage of 50 mg/kg (mean ± SD, $n = 6$)

increase). The enhancement of bioavailability may be explained by the increasing solubility of osthole, as well as the prolonged mean residence time (MRT) due to the sustained release property of S-SMEDDS. The MRT of the S-SMEDDS increased by 3.01 times and 2.04 times compared with suspension and the L-SMEDDS, respectively, which improved the half-life ($t_{1/2}$) and the absorption time of the drug in rabbits. Therefore, the S-SMEDDS of osthole showed a clear advantage over suspension and L-SMEDDS in improving the oral bioavailability of the drug.

CONCLUSIONS

In this study, a new osthole S-SMEDDS which contained castor oil, Cremophor RH40, and 1,2-propylene glycol was successfully obtained by spherical crystallization technique and evaluated. The morphology, particle size, zeta potential, and self-emulsification time indicated that the prepared S-SMEDDS was stable and reproducible. The optimal formulation consisted of EC and Eudragit S100 in ratio of 1:2 as polymers. Anhydrous ethanol to dichloromethane in the ratio of 5:3 was required as good solvent and bridging agent respectively. Besides, the optimal volume of 0.08% SDS aqueous solution used as poor solvent was found to be 120 mL. The formulation was stirred at a screw speed of 400 rpm for 35 min under 25°C. Prepared osthole S-SMEDDS presented high yield and encapsulation efficiency. The *in vitro* release study of the osthole S-SMEDDS revealed a sustained release effect best described by first-order kinetics. Stability test suggested the preparation was stable at low temperature in dark and sealed environment. Importantly, *in vivo* pharmacokinetics study showed that the osthole S-SMEDDS significantly increased the oral bioavailability compared with drug suspension or L-SMEDDS in rabbits. Based on these facts, osthole S-SMEDDS successfully addressed the low solubility and oral bioavailability of the drug, which could potentially expand the drug applications in clinical settings.

Table IV. Pharmacokinetic Parameters of Osthole S-SMEDDS in Comparison with Osthole L-SMEDDS and Osthole Suspension After a Single Oral Administration of 50 mg/kg (Mean ± SD, $n = 6$)

Parameters	Suspension	L-SMEDDS	S-SMEDDS
$MRT_{(0\text{-}t)}$ (h)	1.56 ± 0.10	2.30 ± 0.10	4.70 ± 0.08
$AUC_{(0\text{-}t)}$ (μg h mL^{-1})	8.21 ± 1.30	11.10 ± 2.05	16.83 ± 2.36
C_{max} (μg/mL)	4.39 ± 0.41	3.86 ± 0.43	3.54 ± 0.20
T_{max} (h)	0.50	1.00	4.00

L-SMEDDS liquid self-microemulsifying drug delivery system, *S-SMEDDS* solid self-microemulsifying drug delivery system

ACKNOWLEDGEMENTS

We thank Dr. Jun Shao of St. John's University for his support in the design and writing of the thesis.

FUNDING INFORMATION

This project was supported by the National Natural Science Foundation of China (no. 81274100, no. 81573615) and Project of Scientific Research Fund of Anhui University of Chinese Medicine (no. 2016zr009).

COMPLIANCE WITH ETHICAL STANDARDS

The animal experiments were approved and supervised by the Animal Experimental Ethical Committee of Anhui Medical University (Hefei, China).

Conflict of Interest The authors declare that they have no conflict of interest.

REFERENCES

1. Fusi F, Sgaragli G, Ha le M, Cuong NM, Saponara S. Mechanism of osthole inhibition of vascular Ca(v)1.2 current. Eur J Pharmacol. 2012;680(1–3):22–7.
2. Xia Y, Kong L, Yao YJ, Jiao YN, Song J, Tao ZY, et al. Osthole confers neuroprotection against cortical stab wound injury and attenuates secondary brain injury. J Neuroinflammation. 2015;12(1):155–65.
3. Chiang CY, Lee CC, Fan CK, Huang HM, Chiang BL, Lee YL. Osthole treatment ameliorates Th2-mediated allergic asthma and exerts immunomodulatory effects on dendritic cell maturation and function. Cell Mol Immunol. 2017;14:1–13.
4. Jiang GQ, Liu J, Ren BY, Tang YW, Owusu L, Li M, et al. Anti-tumor effects of osthole on ovarian cancer cells in vitro. J Ethnopharmacol. 2016;193:368–76.
5. Zhang ZR, Leung W, Li G, Kong S, Lu X, Wong Y, et al. Osthole enhances osteogenesis in osteoblasts by elevating transcription factor osterix via cAMP/CREB signaling in vitro and in vivo. Nutrients. 2017;9(6):588–602.
6. Zhang ZR, Leung WN, Li G, Lai YM, Chan CW. Osthole promotes endochondral ossification and accelerates fracture healing in mice. Calcif Tissue Int. 2016;99(6):649–60.
7. Zhang ZR, Leung WN, Cheung HY, Chan CW Osthole: a review on its bioactivities, pharmacological properties and

potential as alternative medicine, Evid Based Complement Alternat Med 2015;2015(2):919616.
8. Hu XB, Liu Y, Bei YY, Zhao J, Zhang XN. Preparation of pH-sensitive osthol-nanoparticles and its pharmacokinetics in rats. Chin J New Drugs. 2012;21(5):490–7.
9. Ma Y, Zhang Y, Zhai Y, Zhu Z, Pan Y, Qian D, et al. Development of a UPLC-TQ/MS approach for the determination of eleven bioactive components in Haizao Yuhu decoction plus-minus Haizao and Gancao drug combination after oral administration in a rat model of hypothyroidism. Molecules. 2016;22(1)
10. An F, Wang SH, Zhang DS, Zhang L, Mu J. Pharmacokinetics of osthole in rabbits. Acta Pharm Sin. 2003;38:571–3.
11. Li Y, Meng F, Xiong Z, Liu H, Li F. HPLC determination and pharmacokinetics of osthole in rat plasma after oral administration of fructus cnidii extract. J Chromatogr Sci. 2005;43:426–9.
12. Hu XJ, Liu Y, Zhou XF, Zhu QL, Bei YY, You BG, et al. Synthesis and characterization of low-toxicity N-caprinoyl-N-trimethyl chitosan as self-assembled micelles carriers for osthole. Int J Nanomedicine. 2013;8:3543–58.
13. Zhang Y, He L, Yue S, Huang Q, Zhang Y, Yang J. Characterization and evaluation of a self-microemulsifying drug delivery system containing tectorigenin, an isoflavone with low aqueous solubility and poor permeability. Drug Deliv. 2017;24(1):632–40.
14. Wu L, Qiao YL, Wang LN, Guo JH, Wang GC, He W, et al. A self-microemulsifying drug delivery system (SMEDDS) for a novel medicative compound against depression: a preparation and bioavailability study in rats. AAPS PharmSciTech. 2015;16(5):1051–8.
15. Zhang JB, Lv Y, Zhao S, Wang B, Tan MQ, Xie HG, et al. Effect of lipolysis on drug release from self-microemulsifying drug delivery systems (SMEDDS) with different core/shell drug location. AAPS PharmSciTech. 2014;15(3):731–40.
16. Bachhav YG, Patravale VB. SMEDDS of glyburide: formulation, in vitro evaluation, and stability studies. AAPS PharmSciTech. 2009;10(2):482–7.
17. Pawar SK, Vavia PR. Rice germ oil as multifunctional excipient in preparation of self-microemulsifying drug delivery system (SMEDDS) of tacrolimus. AAPS PharmSciTech. 2012;13(1):254–61.
18. Singh AK, Chaurasiya A, Awasthi A, Mishra G, Asati D, Khar RK, et al. Oral bioavailability enhancement of exemestane from self-microemulsifying drug delivery system (SMEDDS). AAPS PharmSciTech. 2009;10(3):906–16.
19. Xing Q, Song J, You XH, Xu DL, Wang KX, Song JQ, et al. Microemulsions containing long-chain oil ethyl oleate improve the oral bioavailability of piroxicam by increasing drug solubility and lymphatic transportation simultaneously. Int J Pharm. 2016;511(2):709–18.
20. Lu J, Obara S, Liu F, Fu W, Zhang W, Kikuchi S. Melt extrusion for a high melting point compound with improved solubility and sustained release. AAPS PharmSciTech. 2017:1–13.
21. Ochi M, Kimura K, Kanda A, Kawachi T, Matsuda A, Yuminoki K, et al. Physicochemical and pharmacokinetic characterization of amorphous solid dispersion of meloxicam with enhanced dissolution property and storage stability. AAPS PharmSciTech. 2016;17(4):932–9.
22. Wang TR, Hu QB, Zhou MY, Xue JY, Luo YC. Preparation of ultra-fine powders from polysaccharide-coated solid lipid nanoparticles and nanostructured lipid carriers by innovative nano spray drying technology. Int J Pharm. 2016;511(1):219–22.
23. Ding W, Hou X, Cong S, Zhang Y, Chen M, Lei J, et al. Co-delivery of honokiol, a constituent of Magnolia species, in a self-microemulsifying drug delivery system for improved oral transport of lipophilic sirolimus. Drug Deliv. 2016;23(7):2513–23.
24. Benival DM, Devarajan PV. In situ lipidization as a new approach for the design of a self microemulsifying drug delivery system (SMEDDS) of doxorubicin hydrochloride for oral administration. J Biomed Nanotechnol. 2015;11(5):913–22.
25. Sangsen Y, Wiwattanawongsa K, Likhitwitayawuid K, Sritularak B, Graidist P, Wiwattanapatapee R. Influence of surfactants in self-microemulsifying formulations on enhancing oral bioavailability of oxyresveratrol: studies in Caco-2 cells and in vivo. Int J Pharm. 2016;498(1–2):294–303.
26. Baek MK, Lee JH, Cho YH, Kim HH, Lee GW. Self-microemulsifying drug-delivery system for improved oral bioavailability of pranlukast hemihydrate: preparation and evaluation. Int J Nanomedicine. 2013;8:167–76.
27. Li F, Hu RF, Wang B, Gui Y, Cheng G, Gao S, et al. Self-microemulsifying drug delivery system for improving the bioavailability of huperzine A by lymphatic uptake. Acta Pharm Sin B. 2017;7(3):353–60.
28. Sermkaew N, Ketjinda W, Boonme P, Phadoongsombut N, Wiwattanapatapee R. Liquid and solid self-microemulsifying drug delivery systems for improving the oral bioavailability of andrographolide from a crude extract of Andrographis paniculata. Eur J Pharm Sci. 2013;50(3–4):459–66.
29. Yi T, Wan J, Xu H, Yang X. A new solid self-microemulsifying formulation prepared by spray-drying to improve the oral bioavailability of poorly water soluble drugs. Eur J Pharm Biopharm. 2008;70(2):439–44.
30. Balakrishnan P, Lee BJ, Oh DH, Kim JO, Hong MJ, Jee JP, et al. Enhanced oral bioavailability of dexibuprofen by a novel solid self-emulsifying drug delivery system (SEDDS). Eur J Pharm Biopharm. 2009;72(3):539–45.
31. Djekic L, Jankovic J, Calija B, Primorac M. Development of semisolid self-microemulsifying drug delivery systems (SMEDDSs) filled in hard capsules for oral delivery of aciclovir. Int J Pharm. 2017;528(1–2):372–80.
32. Cole ET, Cade D, Benameur H. Challenges and opportunities in the encapsulation of liquid and semi-solid formulations into capsules for oral administration. Adv Drug Deliv Rev. 2008;60(6):747–56.
33. Cheng G, Hu RF, Ye L, Wang B, Gui Y, Gao S, et al. Preparation and in vitro/in vivo evaluation of puerarin solid self-microemulsifying drug delivery system by spherical crystallization technique. AAPS PharmSciTech. 2016;17(6):1336–46.
34. Hu R, Zhu J, Ma F, Xu X, Sun Y, Mei K, et al. Preparation of sustained-release silyb in microspheres by spherical crystallization technique. J Chin Pharm Sci. 2006;15(2):83–91.
35. Kawashima Y, Cui F, Takeuchi H, Niwa T, Hino T, Kiuchi K. Improved static compression behaviors and tablettabilities of spherically agglomerated crystals produced by the spherical crystallization technique with a two-solvent system. Pharm Res. 1995;12(7):1040–4.
36. Nokhodchi A, Maghsoodi M. Preparation of spherical crystal agglomerates of naproxen containing disintegrant for direct tablet making by spherical crystallization technique. AAPS PharmSciTech. 2008;9(1):54–9.
37. Maghsoodi M, Hassan-Zadeh D, Barzegar-Jalali M, Nokhodchi A, Martin G. Improved compaction and packing properties of naproxen agglomerated crystals obtained by spherical crystallization technique. Drug Dev Ind Pharm. 2007;33(11):1216–24.
38. Niwa T, Takeuchi H, Hino T, Itoh A, Kawashima Y, Kiuchi K. Preparation of agglomerated crystals for direct tabletting and microencapsulation by the spherical crystallization technique with a continuous system. Pharm Res. 1994;11(4):478–84.
39. Chatterjee A, Gupta MM, Srivastava B. Spherical crystallization: a technique use to reform solubility and flow property of active pharmaceutical ingredients. Int J Pharm Investig. 2017;7(1):4–9.
40. Maghsoodi M. How spherical crystallization improves direct tableting properties: a review. Adv Pharm Bull. 2012;2(2):253–7.
41. Sternig A, Müller M, McCallum M, Bernardi J, Diwald O. BaO clusters on MgO nanocubes: a quantitative analysis of optical-powder properties. Small. 2010;6(4):582–8.
42. Mangal S, Meiser F, Tan G, Gengenbach T, Denman J, Rowles MR, et al. Relationship between surface concentration of L-leucine and bulk powder properties in spray dried formulations. Eur J Pharm Biopharm. 2015;94:160–9.
43. Maghsoodi M. Effect of process variables on physicomechanical properties of the agglomerates obtained by spherical crystallization technique. Pharm Dev Technol. 2011;16(5):474–82.
44. Wang XQ, Dai JD, Chen Z, Zhang T, Xia GM, Nagai T, et al. Bioavailability and pharmacokinetics of cyclosporine A-loaded pH-sensitive nanoparticles for oral administration. J Control Release. 2004;97(3):421–9.

45. Hashem FM, Nasr M, Fathy G, Ismail A. Formulation and in vitro and in vivo evaluation of lipid-based terbutaline sulphate bi-layer tablets for once-daily administration. AAPS PharmSciTech. 2016;17(3):727–34.
46. Maity S, Sa B. Compression-coated tablet for colon targeting: impact of coating and core materials on drug release. AAPS PharmSciTech. 2016;17(2):504–15.
47. Sharma VD, Akocak S, Ilies MA, Fassihi R. Solid-state interactions at the core-coat interface: physicochemical characterization of enteric-coated omeprazole pellets without a protective sub-coat. AAPS PharmSciTech. 2015;16(4):934–43.
48. Maghsoodi M, Esfahani M. Preparation of microparticles of naproxen with Eudragit RS and talc by spherical crystallization technique. Pharm Dev Technol. 2009;14(4):442–50.
49. Kachrimanis K, Nikolakakis I, Malamataris S. Spherical crystal agglomeration of ibuprofen by the solvent-change technique in presence of methacrylic polymers. J Pharm Sci. 2000;89(2):250–9.
50. Maghsoodi M, Sadeghpoor F. Preparation and evaluation of solid dispersions of piroxicam and Eudragit S100 by spherical crystallization technique. Drug Dev Ind Pharm. 2010;36(8):917–25.
51. Dixit AR, Rajput SJ, Patel SG. Preparation and bioavailability assessment of SMEDDS containing valsartan. AAPS PharmSciTech. 2010;11(1):314–21.